Morphological Disparity of Ammonoids and the Mark of Permian Mass Extinctions

Loïc Villier[1,2]* and Dieter Korn[2]

The taxonomic diversity of ammonoids, in terms of the number of taxa preserved, provides an incomplete picture of the extinction pattern during the Permian because of a strongly biased fossil record. The analysis of morphological disparity (the variety of shell shapes) is a powerful complementary tool for testing hypotheses about the selectivity of extinction and permits the recognition of three distinct patterns. First, a trend of decreasing disparity, ranging for about 30 million years, led to a minimum disparity immediately before the Permian-Triassic boundary. Second, the strongly selective Capitanian crisis fits a model of background extinction driven by standard environmental changes. Third, the end-Permian mass extinction operated as a random, nonselective sorting of morphologies, which is consistent with a catastrophic cause.

The extinctions at the close of the Paleozoic were initially understood as a relatively long process ranging for about 10 million years (My) or more, recording a progressive decline in numerous groups of marine organisms, many of which became extinct before the end-Permian (*1*). Most recent studies emphasize an "instantaneous" extinction event at geological scales—that is, restricted to the several thousand years bracketing the Permian-Triassic boundary (*2*, *3*)—with a distinct mass extinction event at the end-Capitanian, 10 My earlier (*2*, *4*).

Testing the several putative cause(s) of these events would require detailed studies of the rate, timing, and selectivity of the extinction patterns. The resulting data would permit rejection of extinction hypotheses that do not fit observed patterns. In particular, extinction selectivity can be tested using a wide array of methods (*5–9*). If we assume that the variety of forms (morphological disparity) reflects the variety of adaptive zones occupied, the analysis of disparity patterns provides a means of differentiating among various extinction models (*10–12*).

Ammonoids are suitable subjects for analyses of extinction dynamics because they show high fluctuations in taxonomic diversity during their history and record numerous extinction events and subsequent recovery (*13*). We analyzed diversity dynamics of ammonoids from a distribution of 1965 species ranging from the Late Carboniferous to the Early Triassic. The data are derived from the GONIAT database, a compendium of Paleozoic species of ammonoids encompassing taxonomy, morphological data, and geographical and stratigraphical occurrences (*14*). The database has been extended to include Early Triassic forms and the most recent systematic developments (*15*).

Zhou *et al.* (*16*) interpreted variations in Late Permian ammonoid diversity (Fig. 1) as multi-episodal extinction near the stage boundary, related to sea-level fluctuations. The end-Permian is characterized by the survival of only two or three genera across the Permian-Triassic boundary (*13*). Pseudo-extinction of several paraphyletic taxa certainly over-

emphasizes the level of extinction, but the Early Triassic forms represent only three surviving superfamilies, the Medlicottiaceae and two in the Ceratitina, implying the demise of three others. However, the measured diversity pattern is strongly constrained by analytical biases and the effect of uneven sampling, preventing a confident interpretation.

Ammonoid species and genera are taxa with a short time range, generally restricted to one stage or part of a stage. This leads to an overestimation of extinction intensity when measured at the stage level. In data for the Permian, taxonomic diversity for particular time intervals is also highly correlated with the number of geographical domains sampled (Spearman rank correlation test, $P = 0.009$ and $P = 0.038$ for genera and species richness, respectively). This indicates that measured diversity is highly sensitive to sampling effort and challenges the reliability of the temporal patterns. The crucial problem is that the critical period of the Late Permian and earliest Triassic (Griesbachian and Dienerian) suffers from a paucity of available fossiliferous sections, which can in itself explain part of the diversity patterns (*17*, *18*).

Analysis of morphological disparity can overcome part of the sampling bias of the fossil record (*19*) and also complements patterns of taxonomic diversity. By focusing on shape differences, morphological disparity is relatively independent of taxonomy and allows the comparison of samples in which a variable proportion of taxa are preserved or sampled (*20*). Estimates of disparity consider the distribution of taxa and proportions of morphological space occupied at successive time intervals.

We constructed an empirical morphospace for Permian and Triassic ammonoids on the

Fig. 1. Patterns of diversity for ammonoids for the interval Late Carboniferous to Early Triassic. The diversity is counted at the stage level; the stratigraphic range of taxa is taken from their first and last occurrence in the fossil record. Error bars indicate square roots of numbers of taxa. Upper panel: Number of superfamilies. Lower panel: Comparison of the number of genera (curve) and the number of regions sampled (histogram). Gray vertical bars indicate the position of mass extinctions at the end of the Capitanian and the end of the Changhsingian.
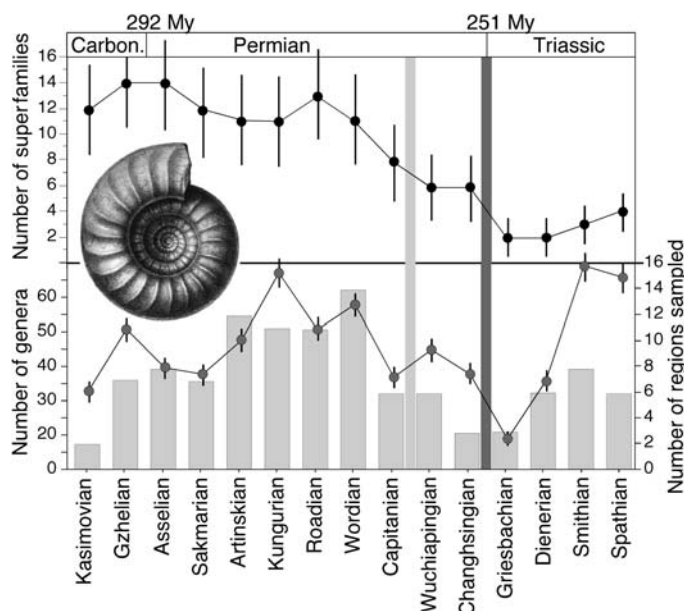
[1]Centre de Sédimentologie–Paléontologie, FRE CNRS 2761, Université de Provence, 3 place Victor-Hugo, F-13331 Marseille Cedex 3, France. [2]Museum für Naturkunde, Humboldt-Universität zu Berlin, Invalidenstraße 43, D-10115 Berlin, Germany.

*To whom correspondence should be addressed. E-mail: lvillier@up.univ-mrs.fr

basis of conch coiling (whorl expansion rate, umbilical width index, whorl width index, and whorl imprint zone). Two complementary estimates of disparity were calculated: the sum of variance and the sum of range on morphospace axes. Variance measures the dispersal of forms through morphospace. It is sensitive to taxonomic choices but is statistically insensitive to the sample size, except in small samples for which uncertainty increases markedly (*12*). The sum of ranges estimates the amount of morphospace occupied. It is insensitive to taxonomic choices but is sensitive to sample size, the impact of which can be minimized with the use of rarefaction (*20*).

The temporal patterns of disparity (Fig. 2) that we found are broadly similar to the diversity curve for superfamilies (Fig. 1) (Spearman rank correlation test, $P = 0.011$). However, at low taxonomic levels, diversity and morphological disparity are independent (no statistical support for correlation, $P = 0.718$ for genera, $P = 0.740$ for species) and track different information. Disparity increased in the Late Carboniferous to Early Permian and remained stable during the first three Permian stages (Fig. 2). During the period from the Artinskian to the end of the Permian (~30 My), disparity decreases, interrupted only by a brief increase in the Wordian. However, patterns of the two disparity estimates differ substantially. Fluctuations in variance are more pronounced, whereas the decreasing trend of the range exhibits more regularity. The brief disparity increase during the Wordian is related to an increase in disparity in three groups [Neoicocerataceae, Adrianitaceae, Cyclolobina (fig. S4)] that diversified during this interval (*14*). The end-Capitanian crisis is characterized by the loss

of a large number of genera (*21*), and the sum of variances decreases more rapidly than does the sum of ranges. The disparity continued to decrease during the two last stages of the Permian and reached the lowest value in the Changhsingian, just before the end-Permian mass extinction. Paradoxically, the level of disparity is similar to that at the beginning of the Triassic, despite a high rate of extinction. The Triassic data show a stagnation in the variance and only a slight expansion of morphospace occupation. The post-crisis diversification of morphologies is delayed relative to the steep increase in taxonomic richness.

According to the models of Foote (*10*), a nonselective extinction should not affect the disparity, whereas selective extinctions should modify the variance and reduce the range (or both), depending on the sensitivity to extinctions among occupants of particular adaptive zones. The progressive long-term decline during the Late Permian—demonstrated by the sum of range, and coeval to the progressive demise of superfamilies—suggests progressive erosion of the morphospace, selectively affecting the marginal morphologies (see fig. S5). This trend is inherent to the ammonoids and reflects a low rate of appearance of morphological novelties that, except for a brief interval in the Wordian, failed to compensate for ongoing background extinction during the Permian. This might be determined either by a constantly filled ecological space or by evolutionary and developmental properties of the organisms (*22*).

The decrease in morphological variance during the Capitanian crisis reflects a reworking of the morphospace whose margins were trimmed back, as expressed by the decrease in

the sum of range, leaving surviving forms mainly clustered in its central part (*21*). The end-Capitanian crisis was thus selective, with most of the cases affecting the goniatitic morphologies (Adrianitaceae, Cyclolobina, Thalassocerataceae) and laterally compressed forms (Medlicottiaceae) (*20*). All these clades suffered during the Capitanian event or became extinct. The Wuchiapingian is distinguished from the Capitanian by the high rate of origination but absence of morphological diversification of the Ceratitina subsequent to the extinction event. Calibrated using conodont biostratigraphy, the end-Capitanian is a relatively long time interval, at least recognizable at a geological scale. Various, but not all, groups of marine organisms were affected, selectively at different times within the end-Capitanian or early Wuchiapingian (*2*). Although treated as occurring at the stage boundary, ammonoid extinction peaked during the earliest Wuchiapingian. The selective extinction of ammonoids and other invertebrate organisms (foraminifers, brachiopods, gastropods) can be attributed to gradual changes in environmental conditions (*2, 5*).

By contrast, the preservation of disparity after the end-Permian mass extinction would be expected only in a context for the nonselective extinctions of whorl morphologies. Although constructed with distinct time scale and taxonomic sampling, the index for suture line complexity (*23*) also provides a measure of morphological disparity of ammonoids. Its changes through time are compatible with a nonselective end-Permian extinction, showing a reduction of the range and the likely preservation of the mean value of the complexity index. Members of the Ceratitina are predominant among the survivors, but this does not reflect selectivity, as they were the taxa most likely to survive. They had the highest morphological disparity and were taxonomically the most diverse group, consisting of more than 100 species (the other clades contained fewer than 10 species each). Simulation using a rarefaction of Changhsingian diversity predicts that the survival of two groups (one being the Ceratitina) has the highest likelihood when 87% of species are randomly killed, which matches previously estimated extinction rates for the end-Permian crisis (*2*).

The end-Capitanian and the end-Changhsingian have been recognized as two distinct mass extinction events, the latter being marked by its intensity, but this model cannot explain all aspects of the end-Permian extinctions. Variation through time of morphological disparity suggests three independent patterns for Permian ammonoids: a long-term reduction in disparity, a high level of selective extinction at the end of the Capitanian, and a nonselective extinction at the end of the Permian. The pattern at the end of the Capitanian corresponds to a model of background extinction

Fig. 2. Patterns of morphological disparity for the ammonoid conch for the interval Late Carboniferous to Early Triassic. (**A**) Disparity estimated as the sum of range measures the amount of morphospace occupied. The values are rarefied to a sample size of 30 species. (**B**) Disparity estimated as the sum of variance approximates the mean dissimilarity between taxa. Plots are the mean value of 500 bootstrap replicates, with 90% confidence intervals as error bars.
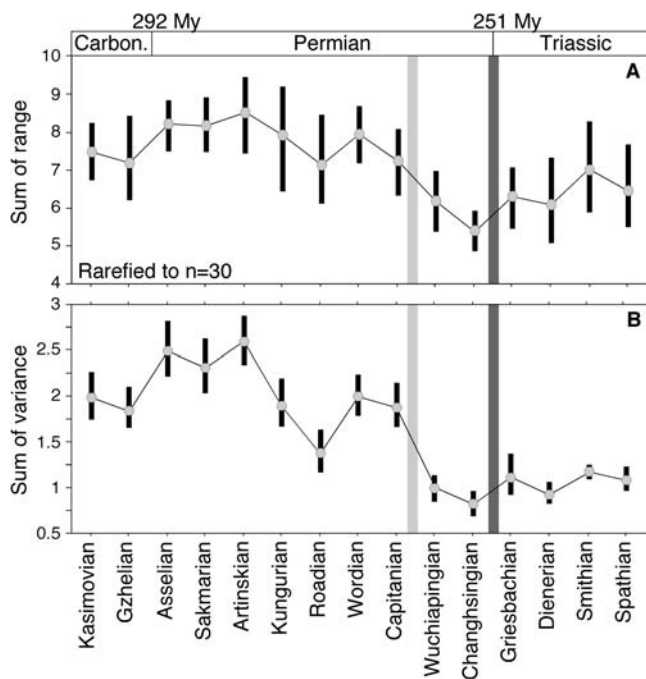
despite the high level of extinction. Only the end-Permian event matches the model of a "mass extinction regime" (5), arguing for a catastrophic cause consisting of a brief but major event, independent of earlier variations in diversity, with a worldwide effect and, for the most part, the nonselective demise of taxa.

References and Notes

1. D. H. Erwin, *The Great Paleozoic Crisis: Life and Death in the Permian* (Columbia Univ. Press, New York, 1993).
2. D. H. Erwin *et al.*, *Geol. Soc. Am. Spec. Pub. 336*, 363 (2002).
3. M. J. Benton, *When Life Nearly Died: The Greatest Mass Extinction of All Time* (Thames & Hudson, London, 2003).
4. S. M. Stanley, X. Yang, *Science* **266**, 1340 (1994).
5. D. Jablonski, *Science* **231**, 129 (1986).
6. D. M. Raup, in *Evolutionary Paleobiology*, D. Jablonski, D. H. Erwin, J. H. Lipps, Eds. (Univ. of Chicago Press, Chicago, 1996), pp. 419–433.
7. A. B. Smith, C. H. Jeffery, *Nature* **392**, 69 (1998).
8. D. Jablonski, *Proc. Natl. Acad. Sci. U.S.A.* **99**, 8139 (2002).
9. M. Aberhan, T. K. Baumiller, *Geology* **31**, 1077 (2003).
10. M. Foote, *Paleobiology* **19**, 185 (1993).
11. K. Roy, M. Foote, *Trends Ecol. Evol.* **12**, 277 (1997).
12. C. N. Ciampaglio, M. Kemp, D. W. McShea, *Paleobiology* **27**, 695 (2001).
13. W. B. Saunders, D. M. Work, S. V. Nikolaeva, *Paleobiology* **30**, 19 (2004).
14. J. Kullmann, D. Korn, *GONIAT Version 3.1, Paleozoic Ammonoid Database System* (Univ. of Tübingen, 2002).
15. T. B. Leonova, *Paleontol. J.* **36** (suppl. 1) (2002).
16. Z. Zhou *et al.*, *Permophiles* **29**, 195 (1996).
17. S. E. Peters, M. Foote, *Paleobiology* **27**, 583 (2001).
18. S. E. Peters, M. Foote, *Nature* **416**, 420 (2002).
19. M. A. Wills, in *Fossils, Phylogeny, and Form—An Analytical Approach*, J. M. Adrain *et al.*, Eds. (Kluwer Academic/Plenum, New York, 2001), pp. 55–144.
20. See supporting data on *Science* Online.
21. B. F. Glenister, W. M. Furnish, in *The Ammonoidea*, M. R. House, J. R. Senior, Eds. (Academic Press, London, 1981), pp. 49–64.
22. C. N. Ciampaglio, *Evol. Dev.* **6**, 260 (2004).
23. W. B. Saunders, D. M. Work, S. V. Nikolaeva, *Science* **286**, 760 (1999).
24. We thank D. Lazarus, D. Unwin, G. J. Eble, and W. Kiessling for discussions. Supported by a postdoctoral fellowship of the Alexander von Humboldt Foundation (L.V.) and by the Deutsche Forschungsgemeinschaft (D.K.). This is Paleobiology Database publication number 28.

The Scaling of Animal Space Use

Walter Jetz,[1,2]*† Chris Carbone,[3] Jenny Fulford,[3] James H. Brown[2]

Space used by animals increases with increasing body size. Energy requirements alone can explain how population density decreases, but not the steep rate at which home range area increases. We present a general mechanistic model that predicts the frequency of interaction, spatial overlap, and loss of resources to neighbors. Extensive empirical evidence supports the model, demonstrating that spatial constraints on defense cause exclusivity of home range use to decrease with increasing body size. In large mammals, over 90% of available resources may be lost to neighbors. Our model offers a general framework to understand animal space use and sociality.

Space use in animals is strongly tied to body size and has been a focal point of ecological research (*1–7*). This research has led to the formulation of scaling rules—power law relations between body size and animal area use—in two separate lines of research: population density and home range size. Here we develop a simple model for the use of space by animals that incorporates energy requirements and interactions with neighbors to unify these approaches.

We assume that energy and material resource requirements are determined by the whole-organism field metabolic rate B (in units of kJ/day or watts), which has been shown to scale as

$$B = B_0 M^{3/4} \qquad (1)$$

[1]Department of Ecology and Evolutionary Biology, Princeton University, Princeton, NJ 08544–1003, USA. [2]Department of Biology, University of New Mexico, Albuquerque, NM 87131, USA. [3]Institute of Zoology, Zoological Society of London, Regent's Park, London, NW1 4RY, UK.

*To whom correspondence should be addressed. E-mail: wjetz@princeton.edu
†Address as of December 2004: Division of Biological Sciences, University of California, San Diego, La Jolla, CA 92093, USA.

B_0 is a normalization constant that also incorporates the diet-specific assimilation efficiency, which determines the proportion of ingested energy available for activity. Let H be the home range area in km² and R the species-specific rate of supply of usable resources available in H, in units of W/km². However, intrusions from foraging conspecific neighbors into a portion of the home range may decrease the proportion of R available to the home range owner (*8*). This resource depletion can be put into a spatial context by thinking in terms of a portion of the home range that is used exclusively only by the owner, H_o, and a portion that overlaps with neighbors and whose resources are harvested only by intruders. We use α to designate the proportion of the resource supply rate across a home range that is harvested exclusively by the owner: $\alpha = H_o R / HR$. This can be simplified to

$$\alpha = H_o/H \qquad (2)$$

Accordingly, the proportion of resource supply rate taken by the neighbors, or home range overlap, is $1 - \alpha$.

It follows that if an individual uses an area just sufficient to meet its metabolic requirements, it requires a home range of area

$$H = B/\alpha R = B_0 R^{-1} \alpha^{-1} M^{3/4} \qquad (3)$$

Population density, N, can be used to empirically quantify α. Its reciprocal, N^{-1}, indicates the average area per individual and is equivalent to H_o, and thus from Eq. 2 it follows that

$$\alpha = N^{-1}/H \qquad (4)$$

Finally, the scaling of N^{-1} is identical to that of H, without the effect of neighbors on scaling and normalization constant

$$N^{-1} = B/R = B_0 R^{-1} M^{3/4} \qquad (5)$$

These equations can serve to illustrate three potential scenarios for the scaling of home range size that are dependent on the examination of the two key parameters, R and α. (i) Both α and R are body size–invariant ($R \propto M^0$ and $\alpha \propto M^0$). This is the hypothesis initially proposed by McNab (*1*). It predicts that home range size should scale as $M^{3/4}$ ($H \propto M^{3/4}$), but it was not supported by subsequent analyses indicating home range scaling close to 1 (*9–12*). (ii) R decreases with body size approximately to the quarter power, whereas α is body size–invariant ($R \propto M^{-1/4}$ and $\alpha \propto M^0$). This predicts the observed $H \propto M^1$. This idea was originally proposed by Harestadt and Bunnell (*13*) and recently refined by Haskell *et al.* (*14*), who modeled the potential interaction between the fractal distribution of resources and foraging mode. This scenario predicts that larger species require larger home ranges than the scaling of their energy needs alone would suggest, because of their lower encounter rates with food items. Because R affects the scaling of both N^{-1} and H equally (compare Eqs. 3 and 5), their scaling lines should have no distinct intersection. (iii) Resource supply rate R does not scale with body size, but proportional access by the home range owner, α, scales approximately to the negative one-